Application of a novel lung protective drug formulated by silver nanoparticles containing *Curcuma longa* L leaf aqueous extract on α-Guttiferin-induced DNA fragmentation and apoptosis in lung HEL 299, MRC-5, IMR-90, CCD-19Lu, WI-38, and BEAS-2B cell lines

Yi Han
Capital Madical University
Yuan Gao
Capital Medical University
Xiaoqing Cao
Capital Medical University
Akram Zangeneh
Razi University
Mohammad Mahdi Zangeneh (m.mehdizangeneh@yahoo.com)
Razi University
Shuku Liu
Capital Medical University
Jie Li
Capital Medical University

Research

Keywords: Lung protective drug, α-Guttiferin, DNA fragmentation, Apoptosis, Silver nanoparticles, Curcuma longa L leaf.

Posted Date: June 17th, 2020

DOI: https://doi.org/10.21203/rs.3.rs-34153/v1

Abstract

Recently, scientists have understood that metallic nanoparticles green-synthesized by medicinal plants have significant anti-cancer effects in the *in vitro*, *in vivo*, and clinical trial conditions. Also, the anti-lung cancer properties of metallic nanoparticles containing natural compounds have been indicated in many studies. In the recent research, we tried to investigate the application of a novel lung protective drug formulated by silver nanoparticles containing *Curcuma longa* L leaf aqueous extract on α-Guttiferin-induced DNA fragmentation and apoptosis in HEL 299, MRC-5, IMR-90, CCD-19Lu, WI-38, and BEAS-2B cell lines. Also, we assessed the concentrations of inflammatory cytokines, activity of caspase-3, and potential of mitochondrial membrane in the *in vitro* condition. Silver nanoparticles were characterized and analyzed by common physicochemical techniques including Transmission Electron Microscopy, Ultraviolet–Visible Spectroscopy, Fourier-Transform Infrared Spectroscopy, and Field Emission-Scanning Electron Microscopy. In the biological part of the present research, the cell viability of HEL 299, MRC-5, IMR-90, CCD-19Lu, WI-38, and BEAS-2B cell lines was measured by trypan blue assay. Caspase-3 activity was assessed by the caspase activity colorimetric assay kit and mitochondrial membrane potential was studied by Rhodamine123 fluorescence dye. Terminal deoxynucleotidyl transferase dUTP nick end labeling (TUNEL) test was used to show DNA fragmentation and apoptosis. Also, the Rat inflammatory cytokine assay kit was used to measure the concentrations of inflammatory cytokines. Silver nanoparticles-treated cell cutlers significantly ($p \leq 0.01$) reduced the DNA fragmentation, caspase-3 activity, and inflammatory cytokines concentrations, and raised the mitochondrial membrane potential and cell viability in the high concentration of α-Guttiferin-treated HEL 299, MRC-5, IMR-90, CCD-19Lu, WI-38, and BEAS-2B cells. The best result of lung protective and antioxidant properties of silver nanoparticles containing *Curcuma longa* L leaf aqueous extract was seen in the high dose of silver nanoparticles i.e., 4 µg. Assessment of the antioxidant properties of silver nanoparticles was done with the common free radical scavenging test i.e., DPPH in the presence of butylated hydroxytoluene as the positive control. The nanoparticles inhibited half of the DPPH molecules in the concentration of 149 µg/mL. According to the above results, silver nanoparticles containing *Curcuma longa* L leaf aqueous extract can be administrated as a lung protective drug for the treatment of lung diseases after approving in the clinical trial studies in humans.

1. Introduction

Metallic nanoparticles are one of main products of nanobiotechnology science. The recent evidences have indicated that metallic nanoparticles have significant therapeutic properties in the *in vitro*, *in vivo*, and clinical trial conditions. Different techniques and approaches were developed to synthesize metallic nanoparticles to make them one of the most applicable and widely used materials in science [1,2]. For instance, silver nanoparticles are used as antioxidants and biocides, and they are utilized either barely or integrated into other structures/substances. Additionally, silver nanoparticles have pharmaceutical and biomedical applications, such as cancer treatment and medical imaging, and not to mention other uses in engineering, cosmetics, and agriculture [2,3]. One crucial branch in nanotechnology is nano-medicine,

which has evolved as an extension for the application of nanomaterials in treating several disorders [3]. Among all nanomaterials, the role of silver nanoparticles green synthesized by medicinal plants as protective and chemotherapeutic supplements in treating various diseases is unique [2].

Several studies have indicated significant antifungal effects of AgNPs green-synthesized by plants in the cure of candida diseases and their antibacterial properties in the treatment of *Streptococcus*, *Staphylococcus*, *Pseudomonas*, *Salmonella*, and *Bacillus* infectious. Also, silver nanoparticles synthesized by plants have been formulated due to the antiviral, antibacterial, antioxidant, anti-parasitic, anti-inflammatory, antifungal, wound healing, and anti-cancer properties [2,3]. In detail, it was reported that silver nanoparticles as useful metallic nanoparticles in medicine, can be used to diagnose several types of lung cancers [3a]. In this regard, Ahmeda *et al.* introduced a chemotherapeutic drug formulated by silver nanoparticles containing *Melissa officinalis* for the treatment of several types of blood cancer [3e]. Another study was showed that silver nanoparticles green-synthesized by *Spinacia oleracea* L. had excellent anti-acute myeloid leukemia. In the previous research, silver nanoparticles significantly removed the leukemia cell lines and regulated the histopathological, immunological, biochemical, and hematological parameters in the animals [3f]. About lung protective properties of silver nanoparticles, Que et al. presented when silver nanoparticles are added to the lung cancer cell lines, ability of lung adenocarcinoma cells (A549) for migrating and metastasis reduce, the levels of reactive oxygen species (RPS) increase, and NF-κB lead to cellular apoptosis. In the previous study was reported the silver nanoparticles with size of more than 100 nm don't have lung protective effects against human lung cancer cell lines. There is a limit studies about the lung protective effects of medicinal plants green-synthesized silver nanoparticles [4]. He et al. reported the lung protective effects of green-synthesized silver nanoparticles on human lung cancer cell (H1299) in the *in vitro* condition. Green-synthesized silver nanoparticles inhibit NF-κB activity, reduce bcl-2 expression, raise survivin and caspase-3 expression and apply remarkable lung protective effects [5].

There is a list of medicinal plants with lung protective effects in traditional medicine including *Acanthopanax senticosus*, *Aconitum tanguticum*, *Alisma orientale* Juzepzuk, *Angelica decursiva*, *Antrodia camphorate*, *Alstonia scholaris*, *Azadirachta indica*, *Callicarpa japonica* Thunb, *Chrysanthemum indicum*, *Cnidium monnieri*, *Eleusine indica*, *Galla chinensis*, *Euterpe oleracea* Mart., *Galla chinensis*, *Ginkgo biloba*, *Gleditsia sinensis*, *Glycyrrhiza uralensis*, *Houttuynia cordata*, *Lonicera japonica* flos, *Morus alba*, *Nigella sativa*, *Paeonia suffruticosa*, *Phellodendri corte*, and *Punica granatum* [6].

In Iranian traditional medicine, many sub-traditional medicines are there that the most well-known is Kurdish traditional medicine in the west of Iran. Every year many medicinal supplements and drugs are formulated and produced from the plants of Kurdish traditional medicine [1–3]. One of these plants is *Curcuma longa* L from *Tracheophytes*, *Angiosperms*, *Monocots*, and *Commelinids* clades, *Zingiberales* order, *Zingiberaceae* family, and *Curcuma* genus [7]. The plant has chemical antioxidant components such as curcumin; curcumadiol; β-phellandrene; terpinolene; β-turmerone; 2,5-dihydroxybisabola-3,10-diene and Procurcumadiol α-turmerone; germacrone-13-al; epiprocurcumenol; procurcumenol; zedoaronediol; isoprocurcumenol; curcumenol; bisacurone; bisacumol; arturmerone; dehydrocurdione; and

curcumenone. In traditional medicine, *Curcuma longa* L is used for its gastroprotective, splenoprotective, hematoprotective, immunoprotective, nephroprotective, hepatoprotective, anti-anemic, antiepileptic, lipid-lowering, anticancer, chemopreventive, diuretic, anti-abscesses, carminative, cutaneous wound healing, pain-killing, antifungal, antipyretic, anti-cataract, antiviral, anti-parasitic, anti-allergic, antiemetic, anti-inflammatory, antidepressant, antifertility, antibacterial, antioxidant, and especially lung protective properties [7]. Maybe, remedial capacities of *Curcuma longa* L are related to the above antioxidant compounds [7].

In the recent research, we decided to investigate the application of a novel lung protective drug formulated by silver nanoparticles containing *Curcuma longa* L on α-Guttiferin-induced cell death in HEL 299, MRC-5, IMR-90, CCD-19Lu, WI-38, and BEAS-2B cell lines.

2. Experimental

2.1. Material

Dimethyl sulfoxide (DMSO), Antimycotic antibiotic solution, hydrolysate, decamplmaneh fetal bovine serum, α-Guttiferin, Ehrlich solution, 4-(Dimethylamino)benzaldehyde, 2,2-diphenyl-1-picrylhydrazyl (DPPH), carbazole reagent, borax-sulphuric acid mixture, Dulbecco's Modified Eagle Medium (DMED), and phosphate buffer solution (PBS) all were achieved from Sigma-Aldrich company of USA.

2.2. Preparation of Curcuma longa L leaf aqueous extract

Fully matured dark green leave of *Curcuma longa* L was collected in Kermanshah province, Iran in January 2020 (Fig. 1). After verification of the colored graphics, identification and characterization processes were performed.

Plant shells were washed with water for a while to remove them from their natural powders. After this procedure, the shells were dried in a sterile environment (botanical laboratory) for 20 days to dry in the natural environment. The next process was to grind these shells into powder.

The obtained powder samples were brought to the appropriate grain size for use and were used in the extraction. Then, 20 g of powder *Curcuma longa* L leaf was taken and added to 500 mL of boiling water and boiled for 5 minutes to obtain the extract. The resulting mixture was centrifuged for 15 minutes at 5000 rpm, then filtered and stored at 4 ^{o}C in the bottle for further experiments [2].

2.3. Synthesis of AgNPs

The AgNPs green synthesis was started with a reaction mixture of 100 mL of $AgNO_3 \times H_2O$ in the concentration of 1×10^{-3} M and 200 mL of *Curcuma longa* L leaf extract (20 µg/mL) in the proportion 1:10 in a conical flask. The reaction mixture was kept under magnetic stirring for 12 h at 25 ^{o}C. The black colored colloidal solution of Ag was formed at the reaction time end.

After centrifuging the mixture at 12000 rpm for 20 min, the supernatant was discarded and the solid sample was washed with abundant pure water. After washing, it was centrifuged again at 1000 rpm for 15 minutes [3].

The characterizations of AgNPs were conducted using advanced spectroscopic techniques like FTIR and UV-Vis spectroscopy, TEM, and FE-SEM.

The presence of AgNPs was primarily confirmed by UV-Vis spectroscopy at 400–700 nm (Jasco V670 Spectrophotometer). The biomolecules that play an effective role in the reduction of AgNPs were investigated by the FT-IR spectrophotometer (Shimadzu IR affinity.1). Morphological properties of silver nanoparticles have been checked concerning structure, form, and thickness by applying FE-SEM and TEM microscopic techniques.

2.4. Lung protective analyses of silver nanoparticles

2.4.1 Cell culture

In this experiment, lung HEL 299, MRC-5, IMR-90, CCD-19Lu, WI-38, and BEAS-2B cell lines were cultured according to protocol rules in the gibco RPMI1640 cell culture environment. In first, 100 IU/mL penicillin (Sigma), 100 µg/mL streptomycin (Sigma) and 10%fetal bovine serum (FBS, Gibco) supported in cell cultures and standard case in T-25cm2 tissue culture bottles (5% incubated at 37ºC in CO_2). It led to changes in the morphology of α-Guttiferin cells, so apoptotic cells led to the cell being treated with diluted α-Guttiferin with 100 mM water.

For $AgNO_3 \times H_2O$, *Curcuma longa* L leaf aqueous extract, and silver nanoparticles solutions in the RPMI1640 water cell cultural environment were first dissolved in DMSO and added to the cultural environment with a final volume of 0.1%. Then, 12 h after the plating and washing, they were classified into several groups including [8]:

1. I) α-Guttiferin: Cell culture contains 100 µM α-Guttiferin.
2. Control: Cell culture medium without α-Guttiferin, $AgNO_3 \times H_2O$, *Curcuma longa* L leaf aqueous extract, and silver nanoparticles.
3. T1: Cell culture contains 100 µM α-Guttiferin and 2 µg of $AgNO_3 \times H_2O$.
4. T2: Cell culture contains 100 µM α-Guttiferin and 4 µg of $AgNO_3 \times H_2O$.
5. T3: Cell culture contains 100 µM α-Guttiferin and 2 µg of *Curcuma longa* L leaf aqueous extract.
6. T4: Cell culture contains 100 µM α-Guttiferin and 4 µg of *Curcuma longa* L leaf aqueous extract.
7. T5: Cell culture contains 100 µM α-Guttiferin and 2 µg of silver nanoparticles.
8. T6: Cell culture contains 100 µM α-Guttiferin and 4 µg of silver nanoparticles.

2.4.2. Cell death index

For determining of cell death index in the various treatments of I-VII, TUNEL staining was used Eight random wells were selected to count TUNEL positive cells with an Olympus AX-70 fluorescence microscope. The ratio of cell death index to apoptotic cells to total cells is equal [9].

2.4.3. Cell viability

Trypan blue was used for assessing cell viability. Vital Dye, whose membranes penetrate broken damaged or Dead Cells, is seen by penetrating dead cells in the Blue lobes in the Neubauer Lamela. For 12 hours, 96 wells with a 5×10^4 cell/mL density were coated on the cultural plate, then, they were cultured with various I-VII treatments and incubated at 37ºC at 5% CO_2 for 48 h. After trypinization of the cells, 200µL of the cell suspension was suspended by Neubauer Lamela 2–3 minutes after mixing with 0.4% 40µL of Trippan blue. The samples cell viability was measured by following the formula below [8].

Cell viability: Non-colored cells number/Total cells number

2.4.4. Caspase-3 activity

For plating the above cells, the well cell culture plate containing the PRMI1640 medium was used. After 12 h, the plate was washed by PBS. Then, the different treatments of I-VII were added to the cells. Trypsin was used for separating the cells from the flask. For removing the supernatant, all samples were centrifuged for 10 minutes. Then the centrifuging was done by adding lysate buffer and finally, they were transferred to the well cell culture plate. Later, 5µL N-acetyl-Asp-Glu-Val-Asp-p-nitroanilineDEVD-pNA was added to the well cell culture plate and incubated in 37ºC for 2 h. Then, releasing of pNA as a result of caspase-3 effect was recorded by Biotek (USA) Spectrophotometer [10].

2.4.5. Mitochondrial membrane potential (MMP)

For half an hour different treatments were exposed to 10 mg / mL rhodamine-123. The cell was then washed using PBS. Subsequently, 900µL triton X-100 was added to each well and held at 4 °C for 2 hours. The solutions were taken into microtubes to be centrifuged at 16000 rpm for 20 minutes. Fluorescent absorbing in cells was performed using a fluorescent microplate reader (488 nm excitation and 520 nm emissions) [10].

2.4.6. Secretion of inflammatory cytokines

The pro-inflammatory cytokines concentrations including TNFα, IL-6, and IL-1β were measured using Rat V-Plex Kit.

2.5 Determination of the antioxidant property of silver nanoparticles

At the beginning of the study, 100 mL of methanol (50%) was added to the 39.4 g of DPPH. Also, several concentrations of $AgNO_3 \times H_2O$, *Curcuma longa* L leaf aqueous extract, and silver nanoparticles i.e., 0-1000 µg/mL, were considered. The DPPH was added to the various concentrations of $AgNO_3 \times H_2O$, *Curcuma longa* L, and AgNPs, and all samples were transferred to an incubator at the temperature of

37 °C. After 30 min incubating, the absorbances were determined at 517 nm. In this study, methanol (50%) and butylated hydroxytoluene (BHT) were negative and positive controls, respectively. Acceding to the following formula, the antioxidant properties of $AgNO_3 \times H_2O$, *Curcuma longa* L leaf aqueous extract, and silver nanoparticles were determined in detail [11]:

$$\text{Presentable DPPH free radical scavenging} = \text{Control} - \frac{Test}{Control} x100$$

2.6. Statistical analysis

The data obtained as a result of experimental studies were evaluated by using the SPSS-22 program and in coordination with Tukeys post hoc process with ANOVA ($p \leq 0.01$).

3. Results And Discussion

3.1. FT-IR analysis

Fourier-transform infrared spectroscopy (FTIR) is the technique used to acquire a solid, liquid or gas infrared spectrum of absorption or emission. Around the same time, an FTIR spectrometer gathers high-specific data across a wide variety of the spectrum. This offers a significant advantage over a dispersion spectrometer, which measures the intensity at a time over a restricted range of wavelengths. Metal-oxygen vibration of the FT-IR spectrum for metal nanoparticular biosynthesis induces peaks that are located at 400 and 700 cm^{-1} [2,3]. The silver nanoparticles formation in the present study confirms by the existence of a peak at 643 cm^{-1} belongs to the Ag-O bending vibration. In the field of natural products, the IR spectroscopic approach is also an appropriate way to identify the bioactive components. Then the technique is a useful tool for identifying the presence of secondary metabolite over silver nanoparticles in the plants. The analysis has shown that in *Curcuma longa* L there are different IR bands related to the presence of different functional groups at 2039 cm^{-1} band related to aliphatic "C-H" stretching; peaks of 3404 cm^{-1} related to "O-H" stretching (For alcohols, carboxylic acids and phenols); peaks of 1127 cm^{-1} could be compared to "-C-O" stretching and peaks of 1379 and 1612 cm^{-1} correspond to "C = C" and "C = O" stretching found in phenolic and flavonoid compounds, respectively (Fig. 2). The explanation for these peaks can be thought to be different compounds from previous research, such as the recorded flavonoid, phenolic and carboxylic compounds [2,3].

3.2. UV-Vis analysis

Ahmeda et al. studied *Melissa officinalis* leaf aqueous extract mediated synthesis of silver nanoparticles. Absorption of the continuum was detected at 462 nm [3e]. Hamelian et al. reported *Thymus kotschyanus* aqueous extract synthesized silver nanoparticles with a peak at 440 nm in the UV-Vis spectrum [3a]. Hemmati et al. recorded 430 nm of the absorption coefficient for silver nanoparticles utilizing the polyol process [3b]. Mohammadi et al. observed the peak of silver nanoparticles containing *Phoenix dactylifera* seed ethanolic extract at the wavelength of 438 nm [3d]. Zangeneh et al. revealed the absorbance at 462 nm for silver nanoparticles synthesized by *Spinacia oleracea* L. [3f]. Hamelian et al. recorded *Pistacia atlantica* leaf extract induced silver nanoparticles as well as absorption maximum was detected at 440 nm [3c].

3.3. FE-SEM analysis

An FE-SEM is an electron microscope (particles that have negative charge), rather than light, which works. Those electrons are emitted through a source of field emissions. The object is scanned by electrons according to a zig-zag pattern and recorded the surface morphology and the size of materials [2,3]. The FE-SEM image of *Curcuma longa* L leaf aqueous extract mediated silver nanoparticles is shown in Fig. 4. The silver nanoparticles appeared as an agglomerated structure. The hydroxyl groups present in *Curcuma longa* L leaf aqueous extract could be responsible for agglomeration [2,3].

In the silver nanoparticles, the range size of 14–27 nm was observed. Many similar observations are noted by Ahmeda *et al*. [3e], Zangneh *et al*. [3f], Hamelian *et al*. [3b], and Mohammadi *et al*. [3d].

3.4. TEM analysis

TEM is the standard tool for calculating the size of nanoparticles, grain size, size distribution, and morphology directly [2,3]. Therefore, TEM analyses of silver nanoparticles were conducted to evaluate particle distributions and mean particle size (Fig. 5). The range size of the nanoparticles calculated through TEM images. Besides, the histogram plot in the TEM image uniformly revealed the particle size distribution of the biosynthesized silver nanoparticles between 14 and 27 nm.

In the previous studies, the size of silver nanoparticles formulated by aqueous extract of medicinal plants had been calculated in the ranges of 10–50 nm with the shape of spherical [2,3]. These literature studies and analyzes support the results of our study and experiment.

3.5. Lung protective potentials of green-synthesized silver nanoparticles

α-Guttiferin is prescribed as a chemical material and may be of concern because of its side effects [12,13]. Abuse of this chemical material may affect the upper respiratory system (including nasal cavity, pharynx, and larynx) and lower respiratory tract (Including trachea, primary bronchi, secondary bronchi, and lung); its metabolites may be harmful to the digestive and excretion system [14,15]. The pathway for the breakdown of α-Guttiferin passes through the liver and kidneys, and consequently, the potential of

side effects is high in these organs [16,17]. In a study, the effects of α-Guttiferin on the lung and brain (cerebral cortex and hippocampus) are revealed. They emphasized the role of oxidative stress, neuronal, and pulmonary damage in the disruptive effects of α-Guttiferin abuse [16–18].

α-Guttiferin has direct effects on the upper and lower respiratory systems and increases the reactive oxygen species (ROS) by reducing the level of antioxidant activity in the plasma. Therefore, it seems necessary to evaluate the toxic effect of α-Guttiferin in upper and lower respiratory systems cells and study on compounds that can decline these toxic effects [16–18].

Different studies have indicated that α-Guttiferin decrease the anti-inflammatory cytokines such as IL13, IL10, IL5, IL4, and IL3 and increases the pro-inflammatory cytokines such as IL1α, IL1β, IL6, and TNFα. The cytotoxicity properties of α-Guttiferin increase cell death significantly and reduce cell proliferation in upper and lower respiratory system cells [15–18]. Also, a study showed that α-Guttiferin through apoptosis induction, caspase-3 and caspase-9 activation, and cell proliferation inhibition induced cell death in cells [17]. The findings of our experiment also agreed with these results and revealed that α-Guttiferin at high concentrations (100 μM) reduced significantly ($p \leq 0.01$) cell viability and increased inflammatory cytokines concentrations and caspase-3 activity. Treatment of these cells with both doses of silver nanopartivles synthesized using *Curcuma longa* L leaf aqueous extract increased the cell proliferation and cell viability potentials due to the cell cytotoxicity reduction (Fig. 6–9).

The previous researches presented that α-Guttiferin produced many free radicals, especially ROS in the body [16–18]. Free radicals with the degradation of DNA molecules cause cellular degradation and apoptosis in the cells [19]. ROS directly damages the DNA and increases the apoptosis in upper and lower respiratory systems cells through the production of free radicals [19–21]. In our study, the experiment of apoptosis by the TUNEL test indicated that α-Guttiferin caused DNA fragmentation and induced apoptosis in lung HEL 299, MRC-5, IMR-90, CCD-19Lu, WI-38, and BEAS-2B cells. Further experiments revealed that α-Guttiferin causes apoptosis in these cells by reducing the mitochondrial membrane potential. Our findings also indicated that silver nanoparticles synthesized using *Curcuma longa* L leaf aqueous extract significantly ($p \leq 0.01$) increased the mitochondrial membrane potential and reduced the rate of DNA fragmentation in lung HEL 299, MRC-5, IMR-90, CCD-19Lu, WI-38, and BEAS-2B cells treated with α-Guttiferin (Fig. 10,11).

3.6. Antioxidant potentials of green-synthesized silver nanoparticles

Traditional medicinal plants are well-known and essential natural antioxidant sources. Medicinal plant-derived natural antioxidants are very efficient in blocking the process of oxidation by neutralizing free radicals. It is also commonly accepted that medicines taken from plant products are safer than their synthetic counterparts; however, the toxicity profile of most medicinal plants have not been comprehensively assessed [22–24]. Combining them with metallic salts is a good option for increasing the antioxidant competencies of therapeutic plants.

In previous studies, a significant increase in antioxidant properties has been reported when produced by green synthesis with salts such as titanium, manganese, cobalt, palladium, gold, zinc, copper and iron[24–26]. So far, significant antioxidant potentials of silver nanoparticles synthesized by many plants such as *Melissa officinalis* leaf, *Thymus kotschyanus* leaf, *Phoenix dactylifera* seed, *Spinacia oleracea* L leaf, and *Pistacia atlantica* leaf were proved [2].

In the study, concentration-dependent DPPH radical scavenging effect of *Curcuma longa* L leaf extract and silver nanoparticles such as BHT was observed. The interaction between *Curcuma longa* L leaf aqueous extract and AuNPs and DPPH may have occurred by transferring electrons and hydrogen ions to the "2,2-diphenyl-1-picrylhydrazyl" radical to form a stable "2,2-diphenhydrazine". ”Molecule (DPPH) [27–32].

The IC50 values of BHT, *Curcuma longa* L leaf aqueous extract, and silver nanoparticles were 141, 272, and 125 µg/mL, respectively (Fig. 12).

The antioxidant property created by *Curcuma longa* L, which is caused by the presence of various antioxidant compounds including curcumin; curcumadiol; β-phellandrene; terpinolene; β-turmerone; 2,5-dihydroxybisabola-3,10-diene and Procurcumadiol α-turmerone; germacrone-13-al; epiprocurcumenol; procurcumenol; zedoaronediol; isoprocurcumenol; curcumenol; bisacurone; bisacumol; arturmerone; dehydrocurdione; and curcumenone, may be thought to be neutralizer for reactive nitrogen species (RNS) and reactive oxygen species (ROS) [7].

It seems that silver nanoparticles green-synthesized by *Curcuma longa* L leaf, due to its antioxidant potential, significantly ($p \leq 0.01$) raised cell viability and mitochondrial membrane potential, and reduced inflammatory cytokines concentrations, caspase-3 activity, and DNA fragmentation in the high concentration of α-Guttiferin-treated lung HEL 299, MRC-5, IMR-90, CCD-19Lu, WI-38, and BEAS-2B cells. Today, antioxidants are introduced as a reducer of cell cytotoxicity because they prevent ROS production and oxidative stresses in the cells [2,3].

4. Conclusion

Curcuma longa L leaf harvested from the Kermanshah city, Iran, was used for synthesizing silver nanoparticles as a suitable and safe material. The synthesized silver nanoparticles were characterized and analyzed by TEM, FE-SEM, and FT-IR and UV-Vis spectroscopy. In the UV-Vis, a clear peak with a wavelength of 439 nm indicated the formation of silver nanoparticles. The presence of many antioxidant compounds with related bonds caused the excellent condition to reduce silver in the silver nanoparticles. FE-SEM and TEM analyses revealed a range size of 14–27 nm of the silver nanoparticles with a spherical shape.

In the biological experiments, we concluded that a high dose of α-Guttiferin causes cell death in lung HEL 299, MRC-5, IMR-90, CCD-19Lu, WI-38, and BEAS-2B cell lines through the induction of cell inflammation and apoptosis. Silver nanoparticles enhanced cell viability in a high dose of α-Guttiferin-treated cells.

They repressed inflammatory cytokines (TNF-α, IL-6, IL1α, and IL-1β) production, mitochondrial membrane disruption, and caspase 3 activity. These events reveal that silver nanoparticles suppressed α-Guttiferin-induced cell death in a dose-dependent manner in lung HEL 299, MRC-5, IMR-90, CCD-19Lu, WI-38, and BEAS-2B cell lines. In the future, silver nanoparticles green-synthesized by *Curcuma longa* L leaf can be consumed for increasing the physiological activity of the respiratory system.

Declarations

Conflict of Interest

The authors declare that there is no conflict of interest.

Acknowledgments

The recent project (Project No: KJ2020CX009) was supported by Tongzhou District Science and Technology Committee (Establishment of a high-throughput screening platform for lead compounds based on organoid lung cancer model supported by Tongzhou District Science and Technology Committee).

References

[1] (a) L. Hagh-Nazari, N. Goodarzi, M.M. Zangeneh, A. Zangeneh, R. Tahvilian, R. Moradi, Stereological study of kidney in streptozotocin-induced diabetic mice treated with ethanolic extract of *Stevia rebaudiana* (bitter fraction), Comp. Clin. Pathol. 26(2) (2017) 455-463. (b) A. Ghashghaii, M. Hashemnia, Z. Nikousefat, M. M. Zangeneh, A. Zangeneh. Wound healing potential of methanolic extract of *Scrophularia striata* in rats, Pharm. Sci. 23(4) (2017) 256–263. (c) R. Moradi, M. Hajialiani, S. Salmani, M. Almasi, A. Zangeneh, M. M. Zangeneh. Effect of aqueous extract of *Allium saralicum* R.M. Fritsch on fatty liver induced by high-fat diet in Wistar rats, Com. Cli. Path. (2018) https://doi.org/10.1007/s00580-018-2834-y. (d) T. Sayyedrostami, P. Pournaghi, S. Ebrahimi Vosta-Kalaeea, M.M. Zangeneh, Evaluation of the wound healing activity of *Chenopodium botrys* leaves essential oil in rats (A short-term study), J. Essent. Oil. Bear. Pl. 21(1) (2018) 164-174. (e) M. Zhaleh, N. Sohrabi, M.M. Zangeneh, A. Zangeneh, R. Moradi, H. Zhaleh, Chemical composition and antibacterial effects of essential oil of *Rhus coriaria* fruits in the west of Iran (Kermanshah), J. Essent. Oil. Bear. Pl. 21(2) (2018) 493-501. (f) H. Sherkatolabbasieh, L. Hagh-Nazari, S. Shafiezadeh, N. Goodarzi, M.M. Zangeneh, A. Zangeneh, Ameliorative effects of the ethanolic extract of *Allium saralicum* R.M. Fritsch on CCl_4-induced nephrotoxicity in mice: A stereological examination, Arch. Biol. Sci. 69(3) (2017) 535-543.

[2] (a) A. Ahmeda, A. Zangeneh, M.M. Zangeneh, Green synthesis and chemical characterization of gold nanoparticle synthesized using Camellia sinensis leaf aqueous extract for the treatment of acute myeloid leukemia in comparison to daunorubicin in a leukemic mouse model. Appl. Organometal. Chem. 33

(2019) e5290. DOI:10.1002/aoc.5290. (b) S. Hemmati, Z. Joshani, A. Zangeneh, M.M. Zangeneh, Green synthesis and chemical characterization of Thymus vulgaris leaf aqueous extract conjugated gold nanoparticles for the treatment of acute myeloid leukemia in comparison to doxorubicin in a leukemic mouse model. Appl. Organometal. Chem. 34 (2020) e5267. DOI:10.1002/aoc.5267. (c) M. Zhaleh, A. Zangeneh, S. Goorani, N. Seydi, M.M. Zangeneh, R. Tahvilian, E. Pirabbasi, In vitro and in vivo evaluation of cytotoxicity, antioxidant, antibacterial, antifungal, and cutaneous wound healing properties of gold nanoparticles produced via a green chemistry synthesis using Gundelia tournefortii L. as a capping and reducing agent. Appl. Organometal. Chem. 33 (2019) e5015. (d) M. Shahriari, S. Hemmati, A. Zangeneh, M.M. Zangeneh, Biosynthesis of gold nanoparticles using Allium noeanum Reut. ex Regel leaves aqueous extract; characterization and analysis of their cytotoxicity, antioxidant, and antibacterial properties. Appl. Organometal. Chem. 33 (2019) e5189. DOI: 10.1002/aoc.5189. (e) M.M. Zangeneh, S. Saneei, A. Zangeneh, R. Toushmalani, A. Haddadi, M. Almasi, A. Amiri-Paryan, Preparation, characterization, and evaluation of cytotoxicity, antioxidant, cutaneous wound healing, antibacterial, and antifungal effects of gold nanoparticles using the aqueous extract of Falcaria vulgaris leaves. Appl. Organometal. Chem. 33 (2019) e5216. DOI: 10.1002/aoc.5216.

[3] (a) M. Hamelian, M.M. Zangeneh, A. Amisama, K. Varmira, H. Veisi, Green synthesis of silver nanoparticles using *Thymus kotschyanus* extract and evaluation of their antioxidant, antibacterial and cytotoxic effects. Appl. Organometal. Chem. 32 (2018) e4458. (b) S. Hemmati, A. Rashtiani, M.M. Zangeneh, P. Mohammadi, A. Zangeneh, H. Veisi, Green synthesis and characterization of silver nanoparticles using *Fritillaria* flower extract and their antibacterial activity against some human pathogens. Polyhedron. 158 (2019) 8-14. (c) M. Hamelian, M.M. Zangeneh, A. Shahmohammadi, K. Varmira, H. Veisi, *Pistacia atlantica* leaf extract mediated synthesis of silver nanoparticles and their antioxidant, cytotoxicity, and antibacterial effects under in vitro condition. Appl. Organometal. Chem. 33 (2019) e5278. DOI:10.1002/aoc.5278. (d) G. Mohammadi, M.M. Zangeneh, A. Zangeneh, Z.M. Siavosh Haghighi, Chemical characterization and anti-breast cancer effects of silver nanoparticles using *Phoenix dactylifera* seed ethanolic extract on 7,12-Dimethylbenz[a] anthracene-induced mammary gland carcinogenesis in Sprague Dawley male rats. Appl. Organometal. Chem. 34 (2020) e5136. DOI:10.1002/aoc.5136. (e) A. Ahmeda, A. Zangeneh, M.M. Zangeneh, Preparation, formulation, and chemical characterization of silver nanoparticles using *Melissa officinalis* leaf aqueous extract for the treatment of acute myeloid leukemia in vitro and in vivo conditions. Appl. Organometal. Chem. 34 (2020) e5378. DOI:10.1002/aoc.5378. (f) M.M. Zangeneh, Green synthesis and formulation a modern chemotherapeutic drug of *Spinacia oleracea* L. leaf aqueous extract conjugated silver nanoparticles; Chemical characterization and analysis of their cytotoxicity, antioxidant, and anti-acute myeloid leukemia properties in comparison to doxorubicin in a leukemic mouse model. Appl. Organometal. Chem. 34 (2020) e5295. DOI:10.1002/aoc.5295.

[4] Y. M. Que, X. Q. Fan, X. J. Lin, X. L. Jiang, P. P. Hu, X. Y. Tonga, Q. Y. Tan, Size dependent anti-invasiveness of silver nanoparticles in lung cancer cells. RSC Adv. 9 (2019) 21134-21138.

[5] Y. He, Z. Du, S. Ma, Y. Liu, D. Li, H. Huang, S. Jiang, S. Cheng, W. Wu, K. Zhang, X. Zheng, Effects of green-synthesized silver nanoparticles on lung cancer cells in vitro and grown as xenograft tumors in vivo. Int J Nanomedicine. 11 (2016) 1879–1887.

[6] H. P. Kim, H. Lim, Y. S. Kwon, Therapeutic Potential of Medicinal Plants and Their Constituents on Lung Inflammatory Disorders. Biomol Ther (Seoul). 25 (2017) 91–104.

[7] A. Niranjan, D. Prakash, Chemical constituents and biological activities of turmeric (Curcuma longa L.) - A review. J. Food. Sci. Technol, 45 (2008) 109–116

[8] W. Strober, Curr. Protoc. Immunol. 111 (2015) 1-3.

[9] A. Byrne, J. Southgate, Brison D, H. Leese, J. Reprod. Infertil. 117 (1999) 97-105.

[10] A. Baracca, G. Sgarbi, G. Solaini, G. Lenaz, Biochim. Biophys. Acta. Bioenerg. 1606 (2003) 137-146.

[11] S.J. Hosseinimehr, A. Mahmoudzadeh, A. Ahmadi, S.A. Ashrafi, N. Shafaghati, N. Hedayati, The radioprotective effect of *Zataria multiflora* against genotoxicity induced by γ irradiation in human blood lymphocytes, Cancer. Biother. Radiopharm. 26(3) (2011) 325-329.

[12] Angiosperm Phylogeny Group. An update of the Angiosperm Phylogeny Group classification for the orders and families of flowering plants: APG III". Botanical Journal of the Linnean Society. 161 (2009) 105–121.

[13] Christenhusz, M. J. M. & Byng, J. W. The number of known plants species in the world and its annual increase". Phytotaxa. 261 (2016) 201–217.

[14] Gustafsson, Mats H. G. Phylogeny of Clusiaceae Based on rbcL sequences", International Journal of Plant Sciences, 163 (2002) 1045–1054.

[15] Stevens, P. F. A revision of the Old World species of Calophyllum (Guttiferae). J. Arnold Arboretum 61 (1980) 117–699.

[16] Ruhfel, B. R., V. Bittrich, C. P. Bove, M. H. G. Gustafsson, C. T. Philbrick, R. Rutishauser, Z. Xi, and C. C. Davis. Phylogeny of the Clusioid Clade (Malpighiales): Evidence from the Plastid and Mitochondrial Genomes. American Journal of Botany 98 (2011) 306–25.

[17] K.V. Rao, P.L. Rao. Antibiotic principles of Garcinia morella: IX. Antimicrobial activity of alpha- & beta-guttiferins & their derivatives. Indian J Exp Biol. 5 (1967) 101-105.

[18] K. Santhanam, P.L. Narasimha Rao. Antibiotic principles of Garcinia morella: 13–Antimicrobial activity and toxicity of alpha 1 and Y-guttiferins and their derivatives. Indian J Exp Biol. 7 (1969) 34-36.

[19] J. Najafian, A. Nasri, M. Etemadifar, F. Salehzadeh, Late Cardiotoxicity in MS Patients Treated with Mitoxantrone. Int. J. Prev. Med. 10 (2019) 211.

[20] R.G. Ghalie, G. Edan, M. Laurent, E. Mauch, S. Eisenman, H.P. Hartung, R.E. Gonsette, M.D. Butine, D.E. Goodkin, Cardiac Adverse Effects Associated With Mitoxantrone (Novantrone) Therapy in Patients With MS. Neurol, 59 (2002) 909-913.

[21] E. Kingwell, M. Koch, B. Leung, S. Isserow, J. Geddes, P. Rieckmann, H. Tremlett. Cardiotoxicity and other adverse events associated with mitoxantrone treatment for MS. Neurol. 74 (2010) 1822-1826.

[22] M. Harshiny, C.N. Iswarya, M. Matheswaran, Biogenic synthesis of iron nanoparticles using Amaranthus dubius leaf extract as a reducing agent. Powder. Technol. 286 (2015) 744-749.

[23] L. Katata-Seru, T. Moremedi, O.S. Aremu, I. Bahadur, Green synthesis of iron nanoparticles using Moringa oleifera extracts and their applications: Removal of nitrate from water and antibacterial activity against Escherichia coli. J. Mol. Liq. 256 (2018) 296-304.

[24] S. Taghavi Fardood, A. Ramazani, Green Synthesis and Characterization of Copper Oxide NanoparticlesUsing CoffeePowder Extract. J. Nanos. 6 (2016) 167-171.

[25] K. Rajesh, B. Ajitha, Y.A.K. Reddy, Y. Suneetha, P.S. Reddy, Assisted green synthesis of copper nanoparticles using Syzygium aromaticum bud extract: Physical, optical and antimicrobial properties. Optik. 154 (2018) 593-600.

[26] P. Kaur, R. Thakur, A. Chaudhury, Biogenesis of copper nanoparticles using peel extract of Punica granatum and their antimicrobial activity against opportunistic pathogens. Green. Chem. Lett. Rev. 9 (2016) 33-38.

[27] S. Reuter, S. C. Gupta, M. M. Chaturvedi, B. B. Aggarwal, Oxidative stress, inflammation, and cancer: how are they linked? Biol Med. 11 (2010) 1603-1616.

[28] D. D. Gultekin, A. A. Gungor, H. Onem, A. Babagil, H. Nadaroglu, Synthesis of copper nanoparticles using a different method: Determination of their antioxidant and antimicrobial activity. J Turk Chem Soc A: Chem. 3 (2016) 623-636.

[29] D. Rehana, D. Mahendiran, R. S. Kumar, A. K. Rahiman, Evaluation of antioxidant and anticancer activity of copper oxide nanoparticles synthesized using medicinally important plant extracts. Biomed Pharmacother. 89 (2017) 1067-1077.

[30] M. Del Mar Delgado-Povedano, V. S. De Medina, J. Bautista, F. Priego-Capote, M. D. De Castro MD, Tentative identification of the composition of Agaricus bisporus aqueous enzymatic extracts with antiviral activity against HCV: A study by liquid chromatography–tandem mass spectrometry in high resolution mode. J Function Foods. 24 (2016) 403-419.

[31] S. C. Jeong, S. R. Koyyalamudi, Y. T. Jeong, C. H. Song, G. Pang, Macrophage immunomodulating and antitumor activities of polysaccharides isolated from Agaricus bisporus white button mushrooms. J Med Food. 1 (2012) 58-65.

[32] R. Sankar, R. Maheswari, S. Karthik, K. S. Shivashangari, V. Ravikumar, Anticancer activity of Ficus religiosa engineered copper oxide nanoparticles. Mat Sci Eng C. 44 (2014) 234-239.

Figures

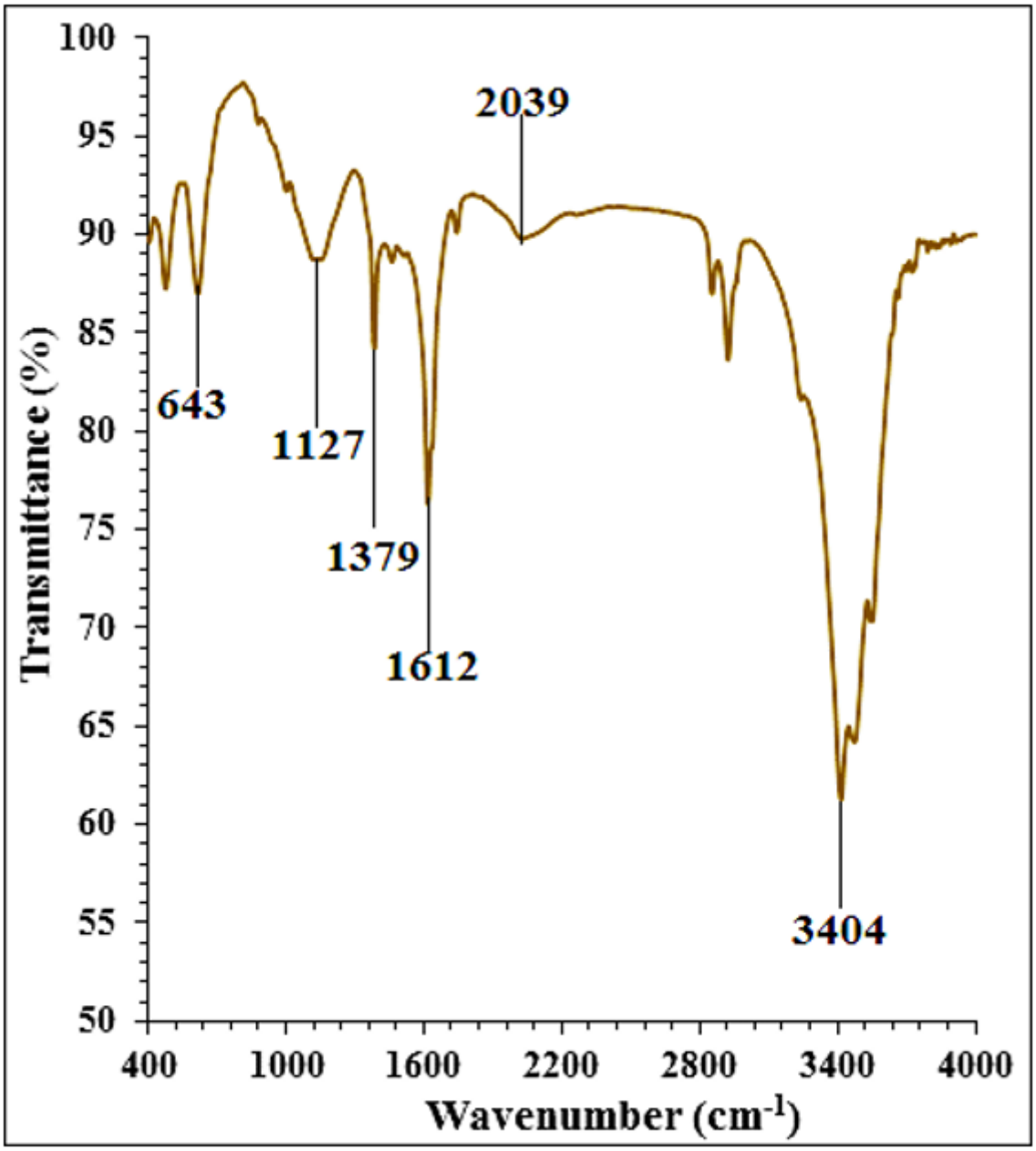

Figure 1

FT-IR analysis of Curcuma longa L leaf aqueous extract silver nanoparticles.

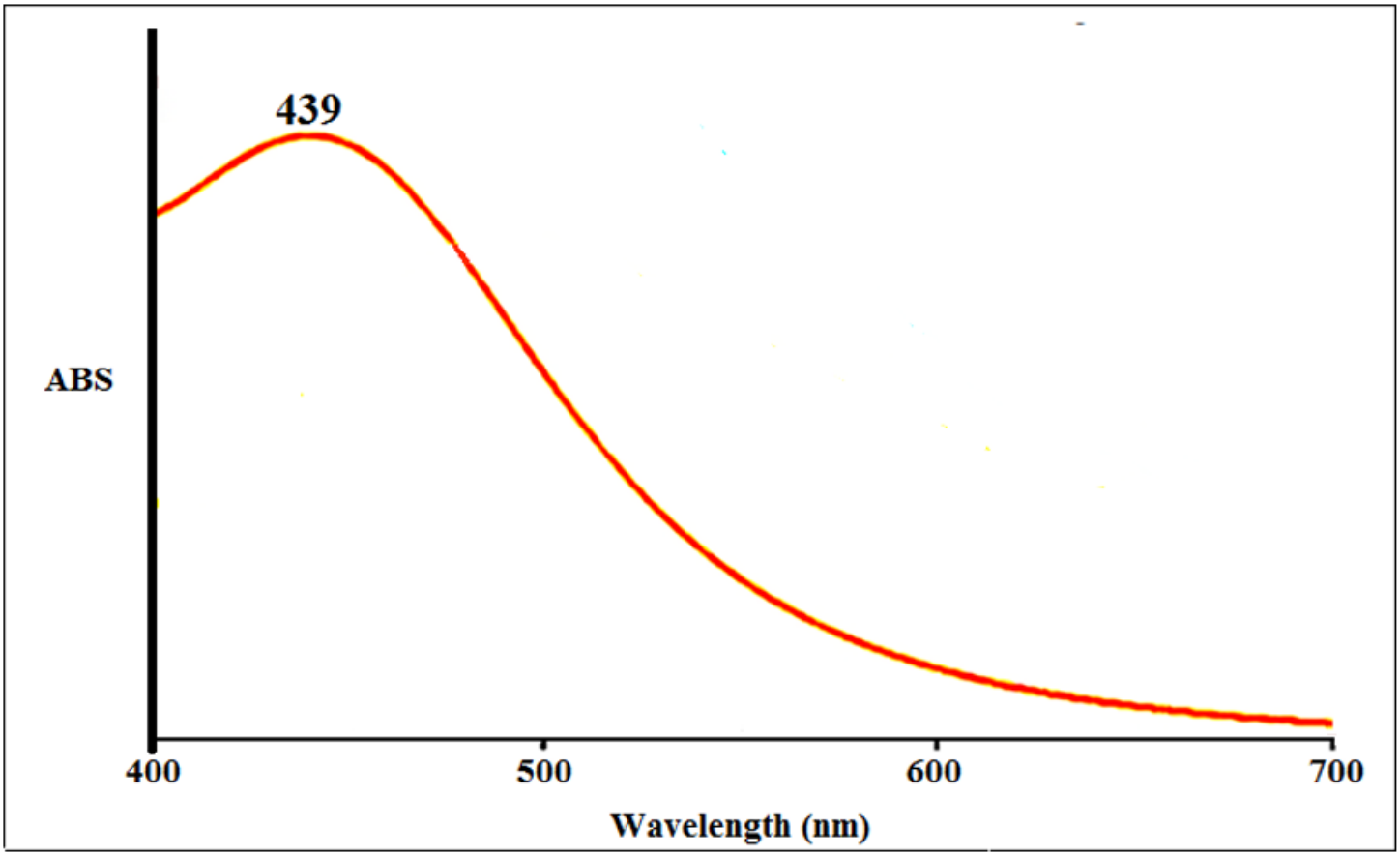

Figure 2

UV-Vis spectroscopy of Curcuma longa L leaf aqueous extract silver nanoparticles.

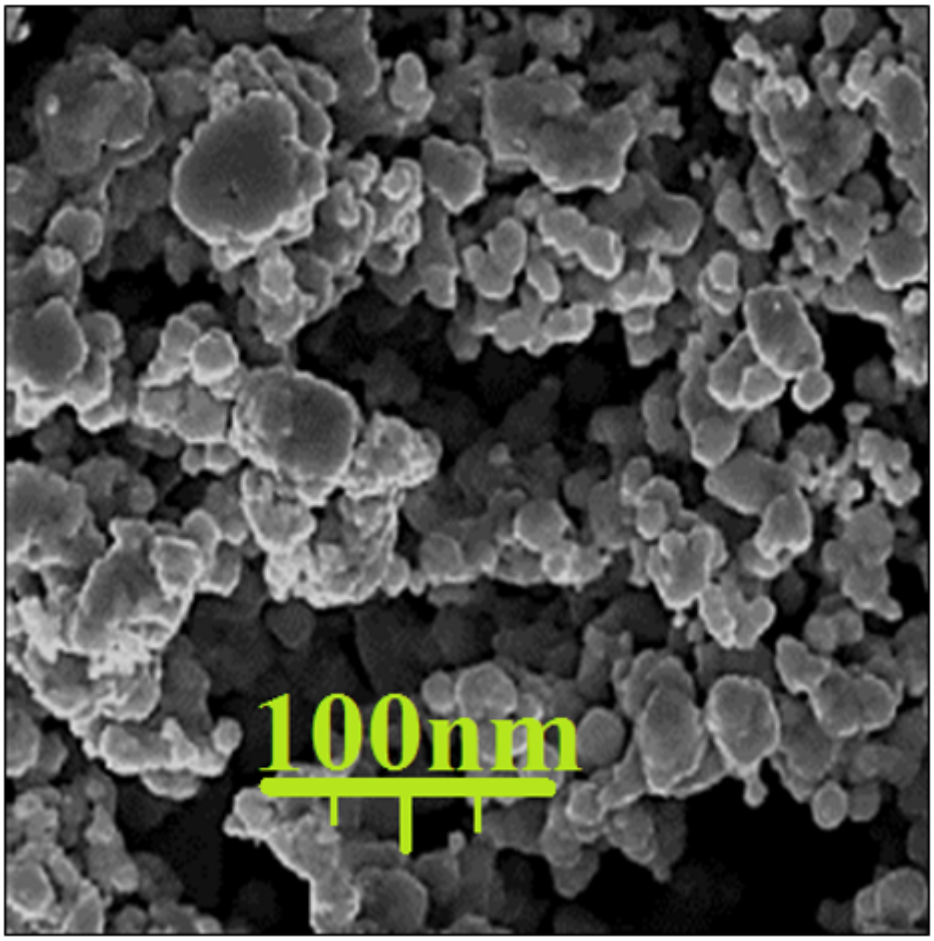

Figure 3

FE-SEM image of Curcuma longa L leaf aqueous extract-silver nanoparticles.

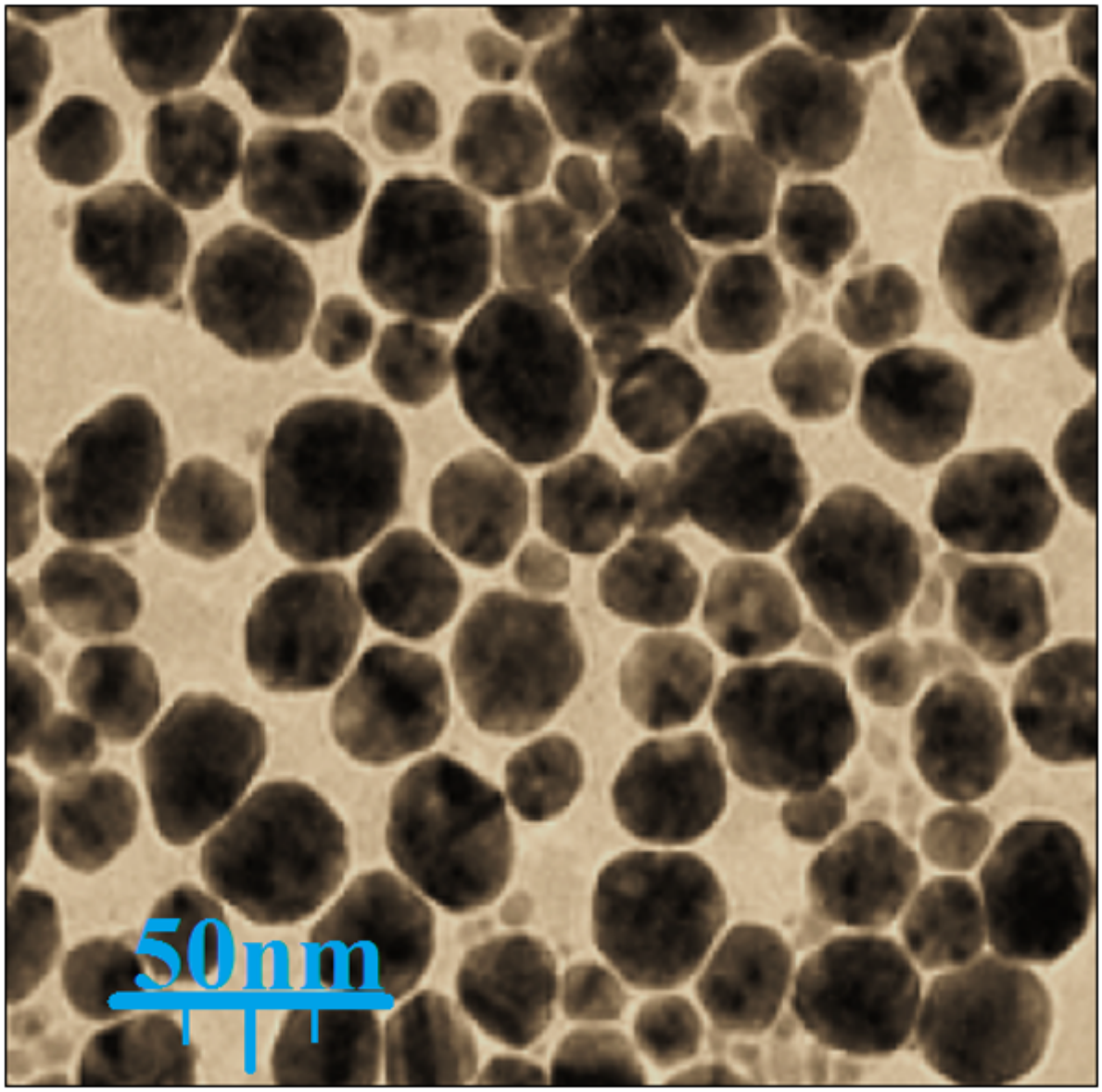

Figure 4

TEM image of Curcuma longa L leaf aqueous extract-silver nanoparticles.

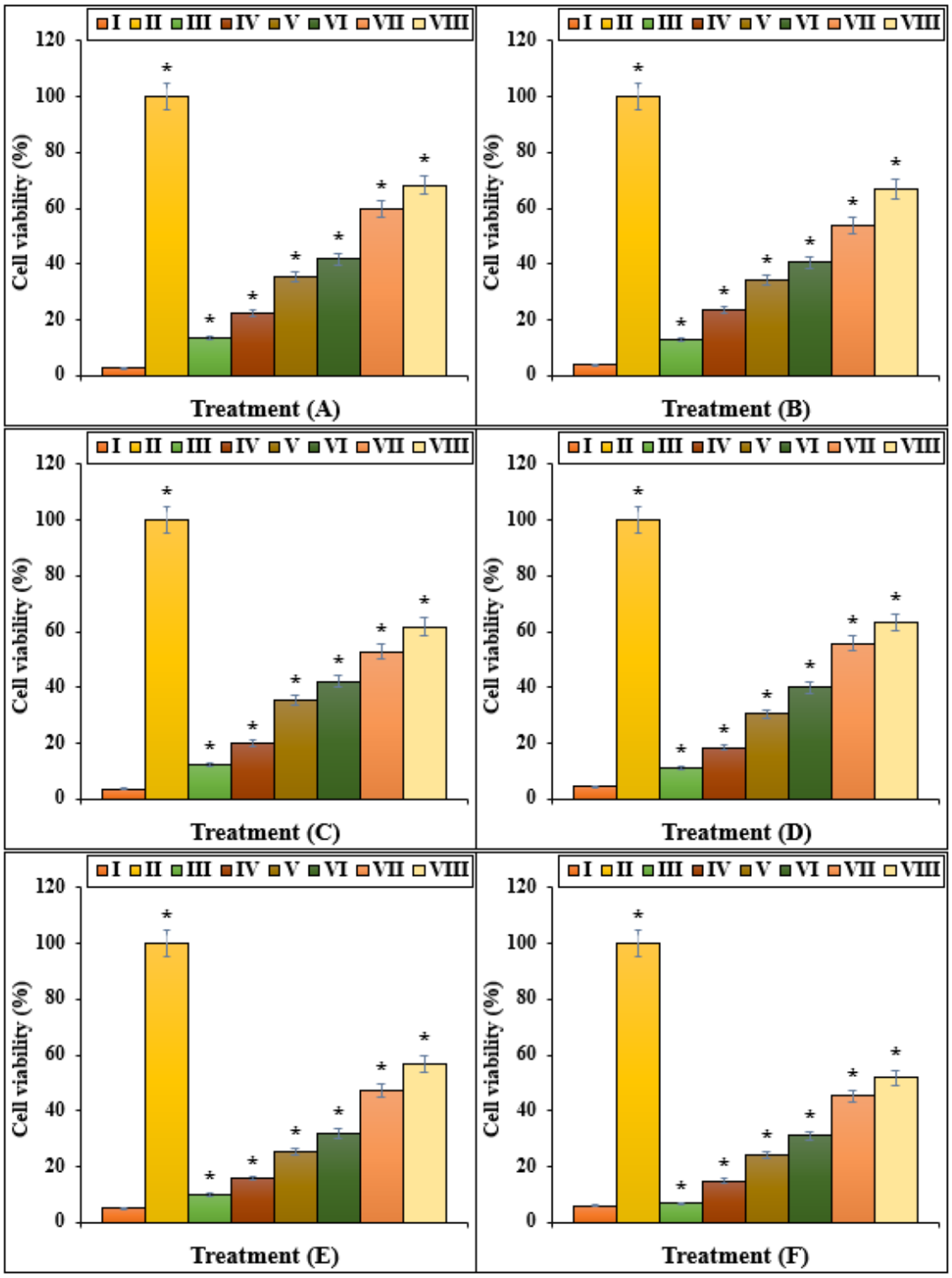

Figure 5

The cell viability of different treatments after 48h. I: α-Guttiferin, II: Control, III: α-Guttiferin and 2 µg AgNO3, IV: α-Guttiferin and 4 µg AgNO3, V: α-Guttiferin and 2 µg Curcuma longa L leaf aqueous extract, VI: α-Guttiferin and 4 µg Curcuma longa L leaf aqueous extract, VII: α-Guttiferin and 2 µg silver nanoparticles, VIII: α-Guttiferin and 4 µg of silver nanoparticles. A: HEL 299, B: MRC-5, C: IMR-90, D: CCD-19Lu, E: WI-38, F: BEAS-2B. *Present remarkable change between α-Guttiferin group and other groups.

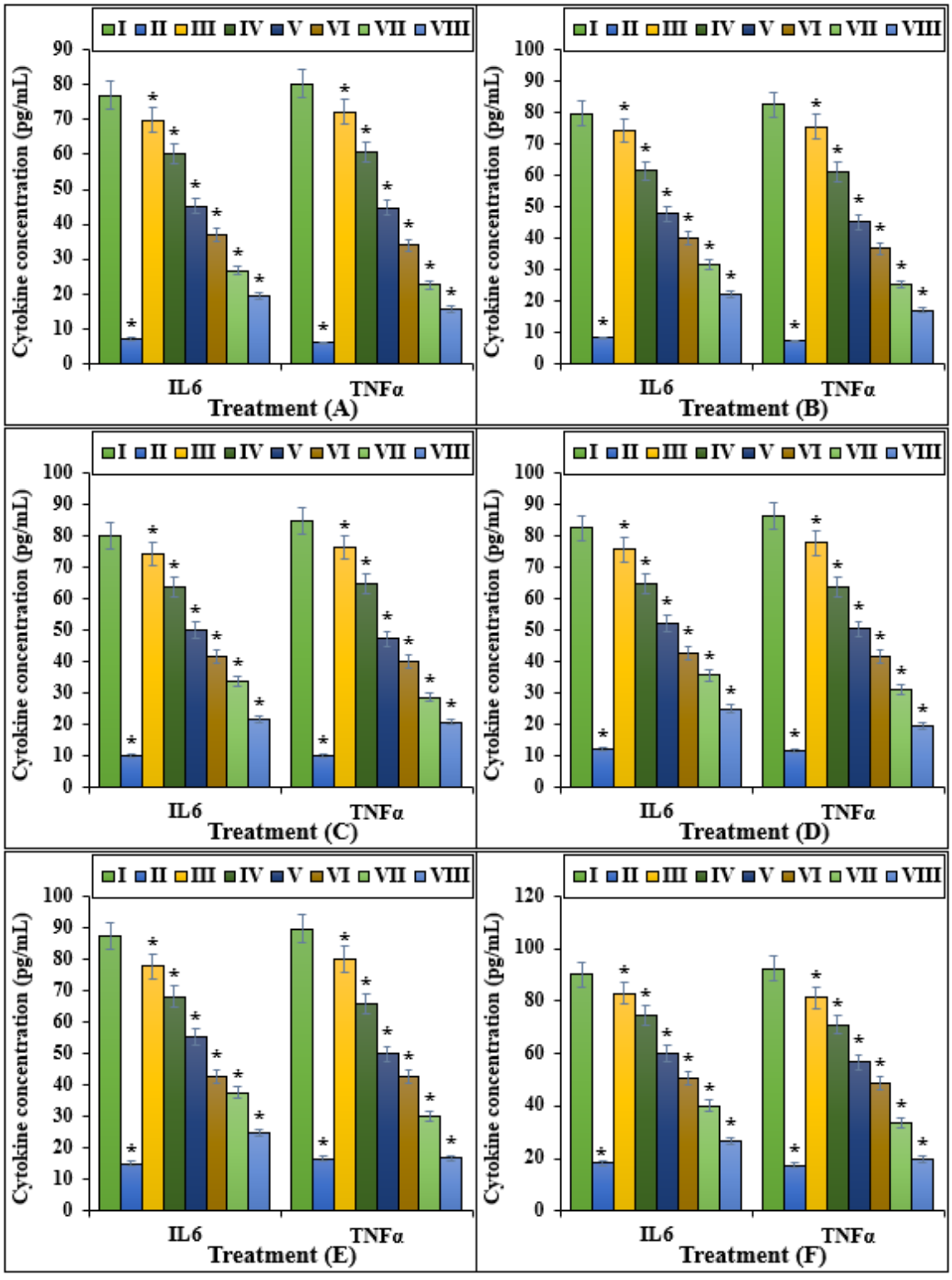

Figure 6

The cytokine concentration (IL6 and TNFα) of different treatments after 48h. I: α-Guttiferin, II: Control, III: α-Guttiferin and 2 µg AgNO3, IV: α-Guttiferin and 4 µg AgNO3, V: α-Guttiferin and 2 µg Curcuma longa L leaf aqueous extract, VI: α-Guttiferin and 4 µg Curcuma longa L leaf aqueous extract, VII: α-Guttiferin and 2 µg silver nanoparticles, VIII: α-Guttiferin and 4 µg of silver nanoparticles. A: HEL 299, B: MRC-5, C: IMR-

90, D: CCD-19Lu, E: WI-38, F: BEAS-2B. *Present remarkable change between α-Guttiferin group and other groups.

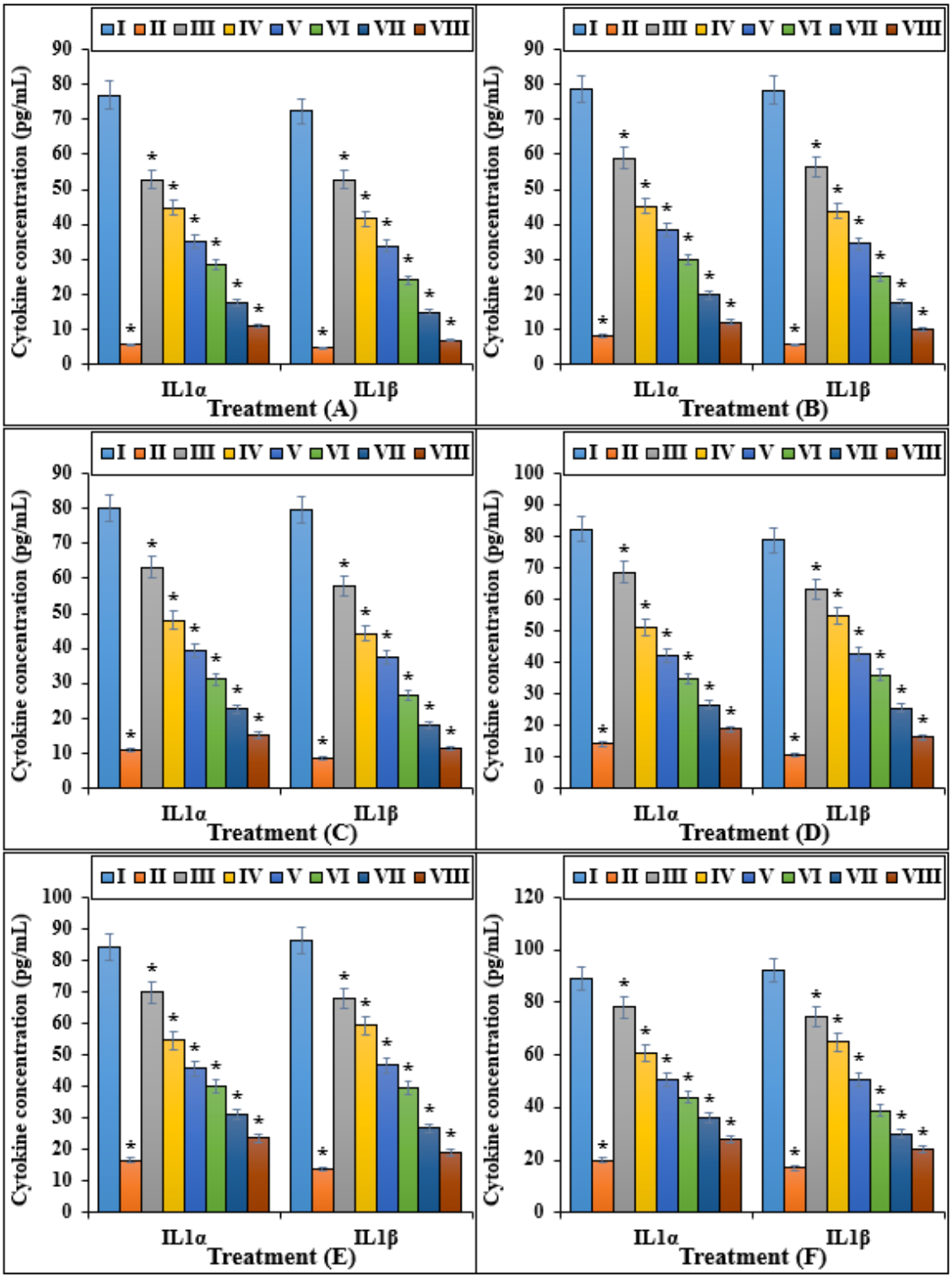

Figure 7

The cytokine concentration (IL1α and IL1β) of different treatments after 48h. I: α-Guttiferin, II: Control, III: α-Guttiferin and 2 µg AgNO3, IV: α-Guttiferin and 4 µg AgNO3, V: α-Guttiferin and 2 µg Curcuma longa L leaf aqueous extract, VI: α-Guttiferin and 4 µg Curcuma longa L leaf aqueous extract, VII: α-Guttiferin and

2 µg silver nanoparticles, VIII: α-Guttiferin and 4 µg of silver nanoparticles. A: HEL 299, B: MRC-5, C: IMR-90, D: CCD-19Lu, E: WI-38, F: BEAS-2B. *Present remarkable change between α-Guttiferin group and other groups.

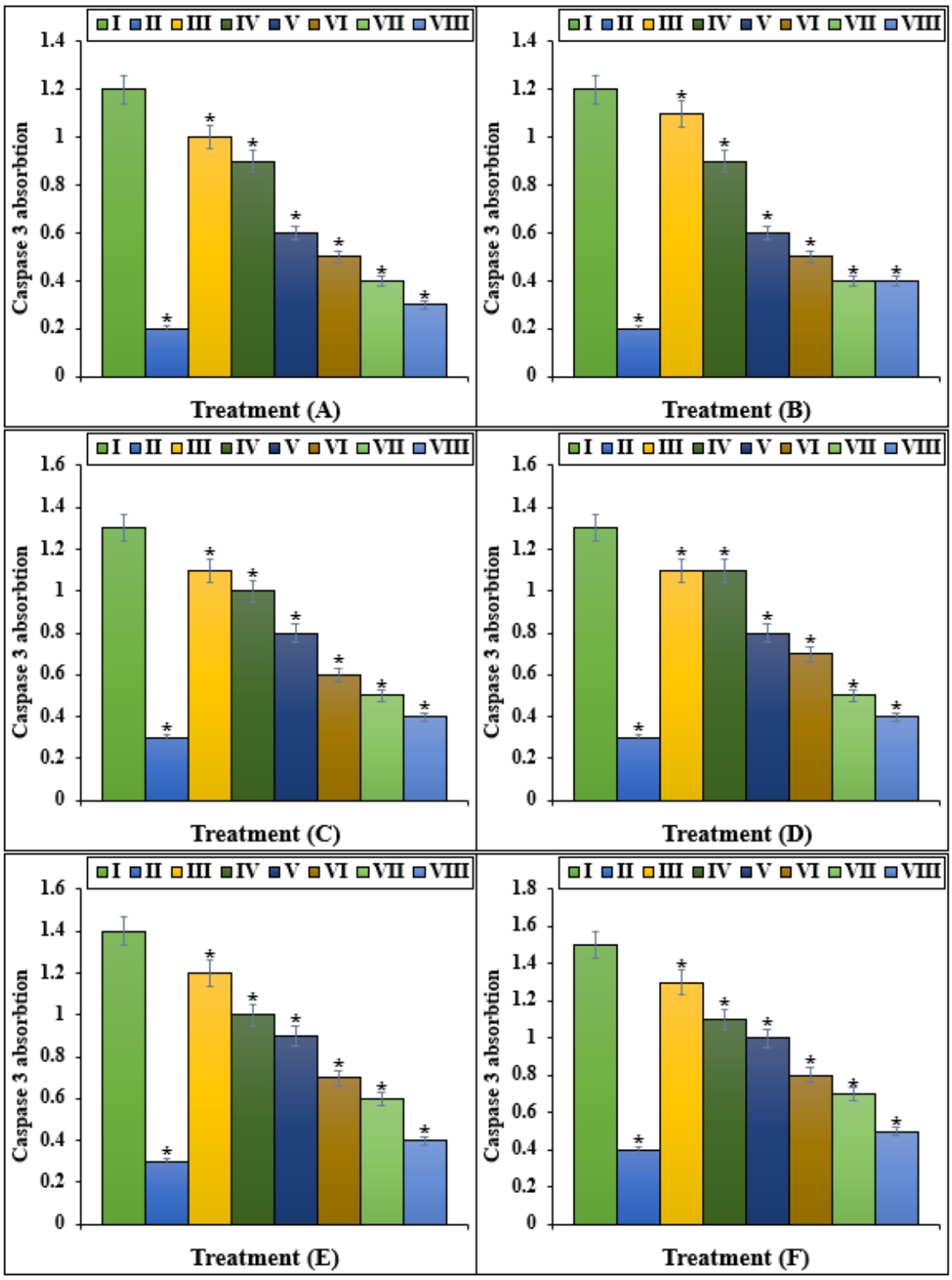

Figure 8

The cytokine concentration (IL1α and IL1β) of different treatments after 48h. I: α-Guttiferin, II: Control, III: α-Guttiferin and 2 µg AgNO3, IV: α-Guttiferin and 4 µg AgNO3, V: α-Guttiferin and 2 µg Curcuma longa L

leaf aqueous extract, VI: α-Guttiferin and 4 µg Curcuma longa L leaf aqueous extract, VII: α-Guttiferin and 2 µg silver nanoparticles, VIII: α-Guttiferin and 4 µg of silver nanoparticles. A: HEL 299, B: MRC-5, C: IMR-90, D: CCD-19Lu, E: WI-38, F: BEAS-2B. *Present remarkable change between α-Guttiferin group and other groups.

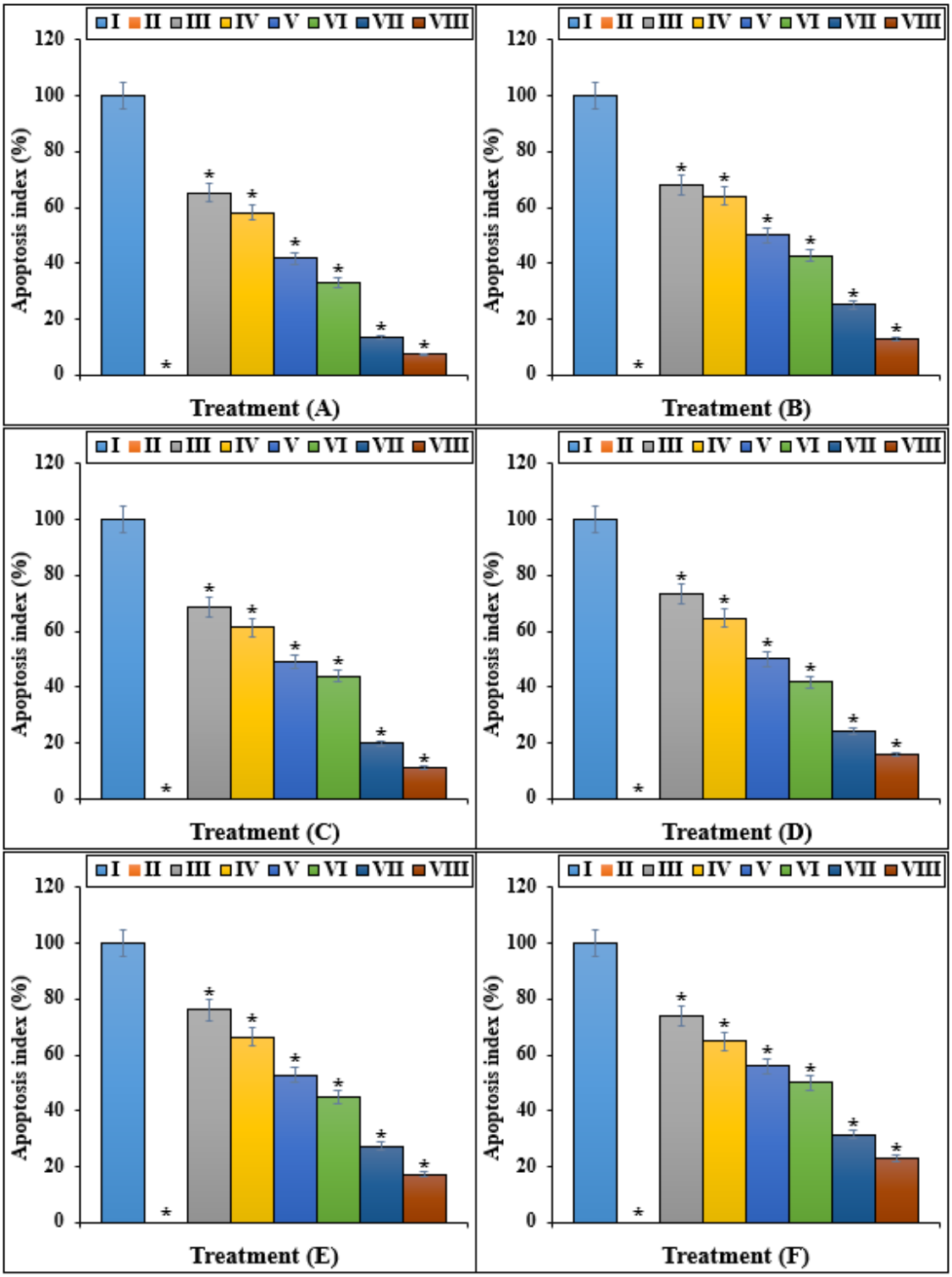

Figure 9

The apoptosis index of different treatments after 48h. I: α-Guttiferin, II: Control, III: α-Guttiferin and 2 µg AgNO3, IV: α-Guttiferin and 4 µg AgNO3, V: α-Guttiferin and 2 µg Curcuma longa L leaf aqueous extract, VI: α-Guttiferin and 4 µg Curcuma longa L leaf aqueous extract, VII: α-Guttiferin and 2 µg silver nanoparticles, VIII: α-Guttiferin and 4 µg of silver nanoparticles. A: HEL 299, B: MRC-5, C: IMR-90, D: CCD-19Lu, E: WI-38, F: BEAS-2B. *Present remarkable change between α-Guttiferin group and other groups.

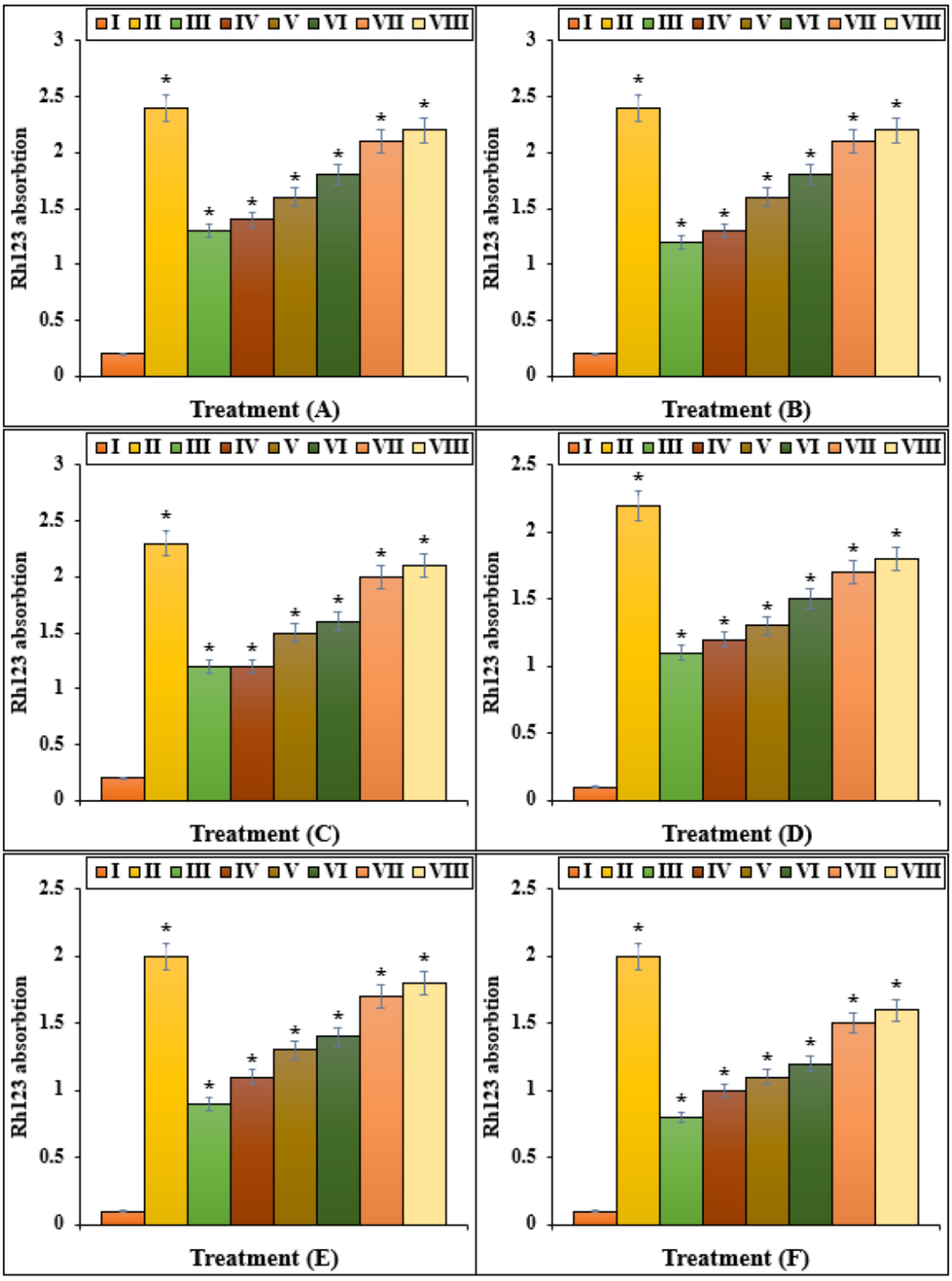

Figure 10

The Rh123 absorption of different treatments after 48h. I: α-Guttiferin, II: Control, III: α-Guttiferin and 2 µg AgNO3, IV: α-Guttiferin and 4 µg AgNO3, V: α-Guttiferin and 2 µg Curcuma longa L leaf aqueous extract, VI: α-Guttiferin and 4 µg Curcuma longa L leaf aqueous extract, VII: α-Guttiferin and 2 µg silver nanoparticles, VIII: α-Guttiferin and 4 µg of silver nanoparticles. A: HEL 299, B: MRC-5, C: IMR-90, D: CCD-19Lu, E: WI-38, F: BEAS-2B. *Present remarkable change between α-Guttiferin group and other groups.

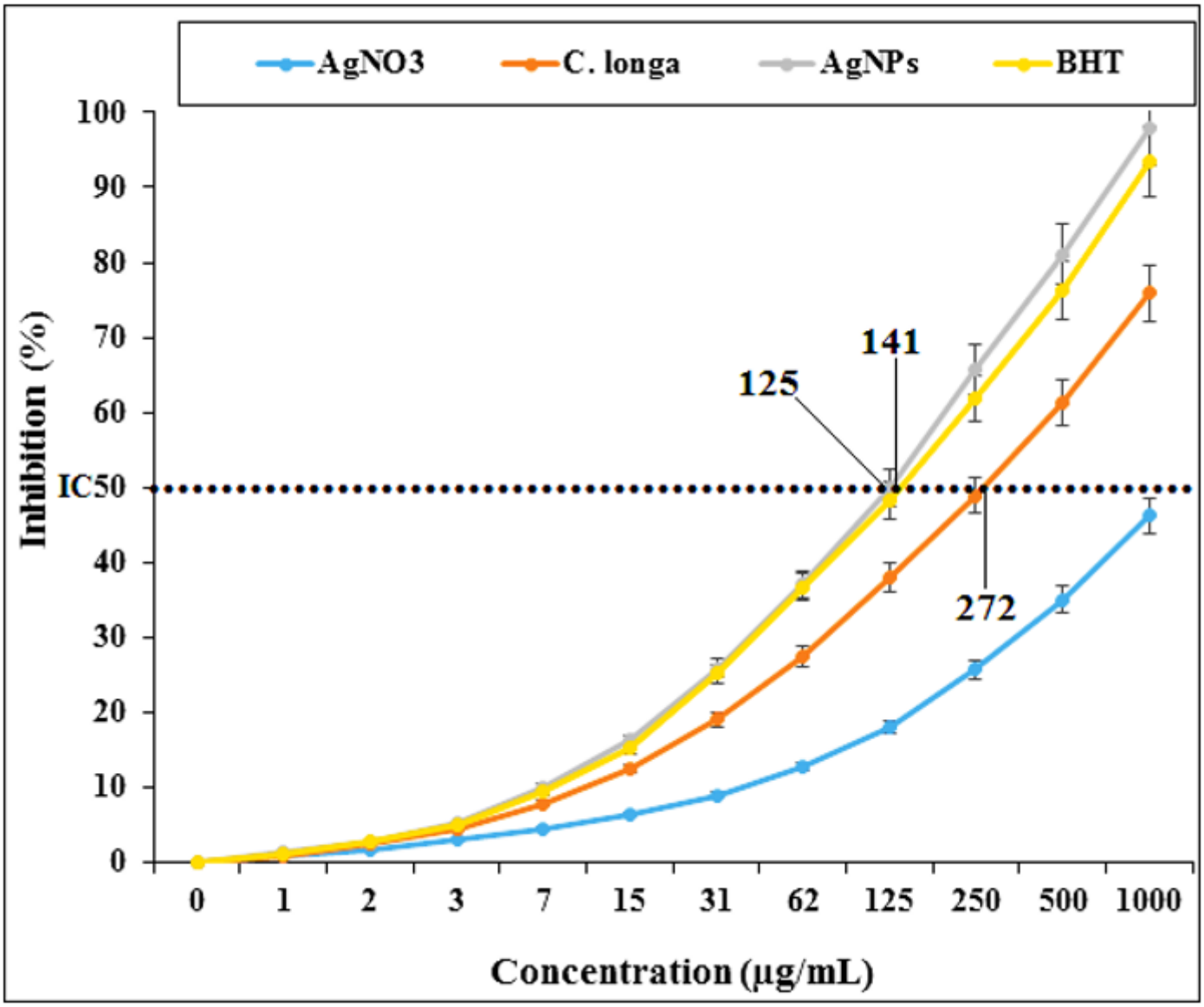

Figure 11

The antioxidant properties of AgNO3, Curcuma longa L leaf aqueous extract, silver nanoparticles, and BHT against DPPH.

Figure 12

The image of Curcuma longa L leaf.